On Satellite Imagery of Land Cover Classification for Agricultural Development

Ali Alzahrani
Department of Computer Engineering, King Faisal University, Saudi Arabia
aalzahrani@kfu.edu.sa

Al-Amin Bhuiyan
Department of Computer Engineering, King Faisal University, Saudi Arabia
mbhuiyan@kfu.edu.sa

Abstract: *Distribution of chronological land cover modifications has attained a vibrant concern in contemporary sustainability research. Information delivered by satellite remote sensing imagery plays momentous role in enumerating and discovering the expected land cover for vegetation. Fuzzy clustering has been found successful in implementing a significant number of optimization problems associated with machine learning due to its fractional membership degrees in several neighbouring constellations. This research establishes a framework on land cover classification for agricultural development. The approach is focused on object-oriented classification and is organized with a Fuzzy c-means clustering over segmentation on CIE L*a*b* colour scheme which provides analysis of vegetation coverage and enhances land planning for sustainable developments. This research investigates the land cover variations of the eastern province of Saudi Arabia throughout an elongated span of period from 1984 to 2018 to recognize the possible roles of the land cover alterations on farming. The Landsat satellite imagery and Geographical Information System (GIS), in tandem with Google Earth chronological imagery are employed for land use variation analysis. Experimental results exhibit a reasonable spread in the cultivated zones and reveal that this Colour Segmented Fuzzy Clustering (CSFC) strategy achieves better than the relevant counterpart approaches considering classification accuracy.*

Keywords: *Satellite imagery, image processing, land cover classification, fuzzy c-means clustering, CIE L*a*b* colour.*

Received January 1, 2021; accepted January 19, 2022
https://doi.org/10.34028/iajit/20/1/2

1. Introduction

Agriculture is the backbone of the national income of most developing countries since it plays a significant impact on economic emancipation and affords the leading source of food, revenue and occupation for the rural populations. Most of the customs and cultures in the world revolve around agriculture. In order to achieve sustainable economic growth, enhancement in agricultural production are necessitate. But agricultural development is strongly associated with the appropriate land cover.

With the proliferation of satellite remote sensing technologies, an enormous amount of high resolution images are now accessible which carry land cover information [18, 20, 21, 31]. But unfortunately, the land cover is not steady for a long over period owing to the human involvements and activities. The residential expansion and land use transformation in city areas have fashioned an urban sprawl for the last few decades. The urbanization in diverse dimensions and perceptions have motivated the rural and industrial developments, culminating in profound effects on the surrounding environment, agglomeration economies, knowledge spill overs and societal climaxing. Recently, the vibrant expansion of urban zones has triggered a snowballing requirement for automatic analysis of terrestrial information in metropolitan areas. Therefore, finding the land cover data from remote sensing imagery and clustering to numerous land cover categories is turning into a thriving research issue [7, 13, 15, 16].

This research provides a framework on land cover classification for agricultural development. The principal purpose of this research is to investigate the land use patterns and monitor the land cover alterations in satellite imagery for administering and planning agricultural areas of Saudi Arabia. Since the government embarked strong national development for the last few decades, Saudi Arabia has endured substantial transformation over land cover towards agriculture [2, 6, 23]. This research investigates the land cover variations of the eastern province of Saudi Arabia during an extensive period from 1984 to 2018 for recognizing the possible roles of the land cover alterations on agriculture. It intends to classify land use types in the specified years: 1984, 1992, 2000, 2008, 2016 and 2018, and determine the modifications that happened in each land use class, and quantify the amount and spread of agricultural land during the three decades. The Landsat satellite imagery and Geographical Information System (GIS), in tandem with Google Earth chronological imagery have been employed for the investigation of land cover variations. The method is based on object-oriented classification and is organized with a Fuzzy c-means

clustering on *CIE L*a*b** colour scheme. Compared to the existing methods, the proposed approach provides substantial improvements to optimize the accuracy depending on the parameters of membership functions. The traditional methods are based on classical set theory, which leads to over-estimation or under-estimation problem. Employing fuzzy set theory in c-means clustering, we could eliminate those problems. This approach provides better result for image clustering over overlapped data sets. Unlike k-means where data point must exclusively belong to one cluster centre here data point is assigned membership to each cluster centre, as a result of which data point belong to more than one cluster centre. This research studied satellite images where land-use practices of buildings, grounds, vegetation, sand dunes and water bodies have been mapped. The ensuing maps revealed that there are suitable land-use and mismanagement practices of land cover for agricultural and residential commitments. This research also provides analysis of satellite images for vegetation coverage and enhances land planning for sustainable developments. Section 2 addresses on related works, Section 3 highlights the materials and methods the used for this research. Section 4 describes the experimental results and discussions. Section 5 presents the overall conclusions and directions for impending research.

2. Related Works

Numerous amounts of research works have been cited in literate on land cover classification employing satellite imagery. Van *et al*. [29] explored the land situated in Nha Trang city in Vietnam over two sensors ALOS/AVNIR-2 and Landsat/OLI&TIR to find the green area by maximum likelihood classification method. Using Markov chain, they predicted that the vegetation cover of the city is in the verge of extinction. Although it is appropriate for application to images with recognised statistical distributions, but the data distribution needs to be assumed in advance. Moreover, the classification outcomes are largely dependent on the designated image features and are sensitive to noise. Phiri [19] outlined a decision tree classification strategy to cluster the remotely sensed satellite images from Landsat 8. They employed a probabilistic approach where object-based image classification was performed through the establishment of rule sets. They developed the decision tree by segregating the spectral dissemination of the training dataset recursively employing the open source data mining software WEKA. They employed pixel-oriented method to investigate the characteristics of every pixel within the range of concern. Since during the investigation, spatial and background information related to these pixels are avoided, this method provide less accuracy.

Memon *et al*. [17] constructed a prototype using deep convolutional neural network for land cover analysis employing Landsat-8 images. Their architecture incorporates cross-channel parametric pooling layer, uses a hierarchical sampling technique for understanding the automatic structure of the training dataset, finds the procedural arrangement of model-related parameters, and finally accomplishes the clustering of remotely sensed data. Although this method perform well where images are identical to the dataset, but it exhibits some limitations if tilted or rotated images are being processed for classification. Khurana and Saxena [14] developed an adaptive procedure with machine learning algorithm to identify the modification in green cover. The algorithm was used on two remote sensing image data sets to cluster the data on alteration and no-alteration groups. They used five texture parameters as input parameters to the classification algorithm. They applied different machine learning approaches to train with different configurations for identifying change on two areas of India. The main drawback of their method is that it is unable to identify the location of different objects in an image. Häme *et al*. [12] have proposed a hierarchical clustering of temporal satellite imaging to determine the abrupt land cover changes. They collected data from different sources, employed an unsupervised clustering scheme and calculated the variation magnitude and variation types for land cover information on calculating the mean intensity values of the lower level groups with their parent cluster means. They validated their methodology by three sets of images. Sentinel-2/Sentinel-2, Landsat 8/Sentinel-2, and Sentinel-2/ALOS 2 PALSAR in a study area of southern Finland. Fan *et al*. [11] developed a convolutional neural network named HRI-RefineNet model to extract various sorts of objects from high-resolution remote sensing images. They classified cultivated land, residential zone, roads and water bodies as detection outputs employing remote sensing imagery. They suggested a modified pooling layer and adjusted the kernel size and number of convolution layers as per the texture features of various objects. Xu *et al*. [30] developed a multi-structure joint decision method for land cover classification employing convolutional neural network. Although these convolutional neural networks attained momentous success due to multi-scale resolution and the advantage of being learning necessary features from a huge data set of training samples, but their networks culminated with abundantly connected layers. They assumed that all pixels in a designated image share the same label and only the centre pixel label is predicted each time. This affects the efficiency of large-scale outcomes and produces inaccurate segmentation, in the verge of the boundary of objects when the input image contains more than one class.

A fair amount of research investigations have been carried out on land cover variations using remotely sensed data in different regions of Saudi Arabia. Most

of the investigations have evaluated the urban development and expansions of city areas in the central, eastern and western regions of Saudi Arabia. These investigations have evaluated GIS information and recognized the increased population to be the prime feature for persuading urban spread in different chronological slots. Al-Harbi [6] investigated on the development of cultivated lands in Tabuk area by computing the Ratio Vegetation Index (RVI) employing Landsat TM and Spot 5 information. He made an assessment on the chronological changes of agricultural land cover during the period from 1988 to 2008. Al-Gaadi *et al*. [5] applied Normalized Difference Vegetation Index (NDVI) on Landsat TM and ETM+ datasets to identify land use variations in Dirab area of Riyadh, Saudi Arabia. Maximum likelihood algorithm was used for image classification in their approaches [5, 6]. The main problem associated with this method is that its computational cost is high. Using multiple images it requires that the training sites must be examined in each of the images, because the land cover may have changed between the two dates. Rahman [22] investigated land cover changes of Riyadh, the capital city of Saudi Arabia employing Landsat data analysis. He detected the urban spread by computing the relative Shannon's entropy metric for the dispersion of low density land cover using the proportion of low density land cover in relation to total land cover. This method suffers from two main problems: it can not be used to compare diversity distributions that have different levels of scale and it cannot be used to compare parts of diversity distributions to the whole. Aljoufie *et al*. [1] investigated on the urban spread of Jeddah, Saudi Arabia employing Landsat Multispectral Scanner (MSS), Landsat Thematic Mapper (TM), and Advanced Spaceborne Thermal Emission and Reflection Radiometer (ASTER) information with an arrangement of aerial images, Satellite Pour l'Observation de la Terre (SPOT) satellite images, and Jeddah's master plan to study the outlines of urban growth during the previous four decades and their associates with the expansion of urban transportation schemes. Alqurashi and Kumar [3] have studied on land cover alteration in Makkah and Al-Taif, Saudi Arabia during the period 1986 to 2013. They employed maximum likelihood classifier on the data obtained from Landset Satellite imagery to develop land cover maps.

Almadini and Hassaballa [2] made an assessment on the spatial and chronological differences of land use in the cultivated zones of the Al-Ahsa region, Saudi, Arabia. Salih [25] has studied on land use information of Al-Ahsa Oasis of Saudi Arabia. Employing Eigen values and Eigen vectors, he calculated the variance of the satellite data and used maximum likelihood classifier to classify the data. He mapped the land cover using Landsat 7 image dataset. Rahman [23] studied on the decadal land cover variations at Al-Khobar, Saudi Arabia employing remote sensing data. He performed land cover classification employing ISODATA clustering strategy on Landsat TM, ETM+, and OLI satellite images over the period 1990 to 2013. He computed the urban spread by measuring the relative Shannon's entropy index and relative entropy standards. Youssef *et al*. [32] employed multispectral satellite imagery to evaluate the chronological progression of farming accomplishments in the Al-Jouf area, Saudi Arabia. These methods are computationally very exhaustive and, therefore, their performances are extremely slow.

The proposed method is based on Fuzzy c-means clustering algorithm which is initiated by assigning the membership to each data point corresponding to each cluster center on the basis of distance between the cluster center and the data point. The more the data is near to the cluster center the more is its membership towards the particular cluster center. Obviously, the summation of membership of each data point should be equal to one. After each iteration membership and cluster centers are updated. This approach provides better result for overlapped data set and obviously better than *k*-means algorithm. Unlike *k*-means where data point must exclusively belong to one cluster center here data point is assigned membership to each cluster center, as a result of which data point belong to more than one cluster center.

3. Materials and Methods

3.1. Study Area

This research has been performed on Al-Ahsa, the largest governate in the eastern province of Saudi Arabia. It is one of the largest oasis in the world with world-renowned date palms which spans an area of 534,000 km^2, and corresponds to approximately 25% of the country's whole area. This region is deliberated as the biggest agricultural zone in Saudi Arabia and is perhaps the largest irrigated oasis in the world [8]. This region is affected by hyper-arid environment, with mean annual rainfall of 80-90 mm, and average temperature of 39°C during summer and 14°C during winter.

Traditionally, agriculture has been the key source of earnings for many years. The area is famous for its palm trees and dates. Customarily life in this region depended on the plentiful water from abundant springs that sustained agriculture, the oasis produced dates, fruit, rice, wheat, and barley [24, 28]. The agricultural area of investigation is located at latitude ranging from 25°12′18"N to 25°46′45"N and longitude from 49°17′29"E to 50°02′8"E (Figure 1).

Images collected from satellites are: December 1984; December 1992, December 2000, December 2008, December 2016, and December 2018 imperative to the study area.

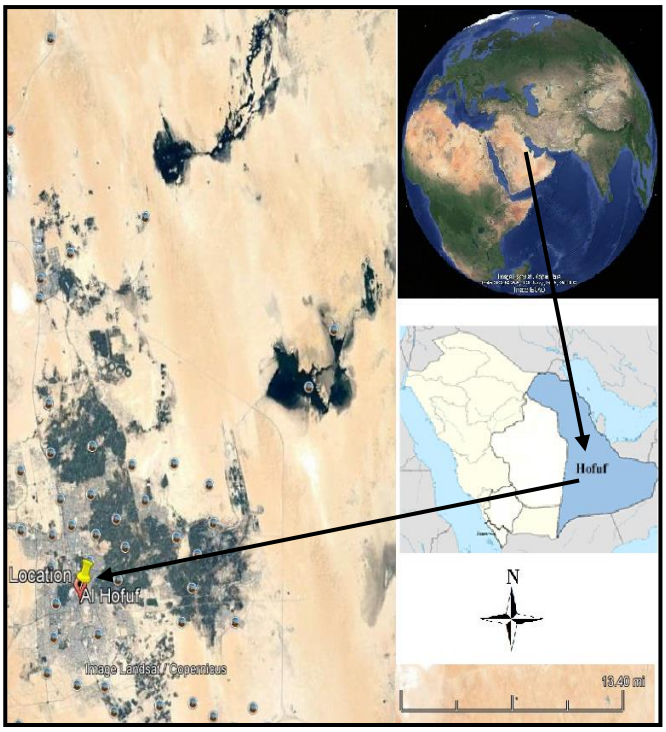

Figure 1. Location of the study area: Hofuf, Saudi Arabia.

3.2. Methods

The method is based on the visual attributes of the *CIE L*a*b* color segmentation and fuzzy clustering approach. It is organized with analyzing the satellite images and the GIS mapping. The overall research has been implemented with a combined procedure to map the numerous chronological variations in the spatial characteristics of the cultivated zones over the period ranging from 1984 to 2018.

3.2.1. Color Segmentation

The color segmentation is achieved by *CIE L*a*b** color scheme. The *CIE L*a*b** color model is defined by three attributes: *L** representing lightness ranging from 0 for black to 1 for white, *a** ranging from green (−) to red (+), and *b** ranging from blue (−) to yellow (+). Since the uniform variations of constituents in the *L*a*b** color scheme intends to resemble approximately the same amount of visually perceived change in color, therefore the relative perceptual discrepancy between any two colors in *L*a*b** is estimated by assuming each color with three constituents: *L**, *a**, *b** and considering the Euclidean distance between them [27].

The *L** value of lightness is expressed by:

$$L^* = 116\, f\left(\frac{Q}{Q_n}\right) \tag{1}$$

Where Q_n is the luminance component for minimal white and f is a finite-slope estimation to the cube root with a value of a=6/29 and expressed by:

$$f(u) = \begin{cases} u^{1/3} & if\ u > \alpha^3 \\ u/(3\alpha^2) + 2\alpha/3 & otherwise. \end{cases} \tag{2}$$

Thus the ensuing [0,100] scale approximately calculates equal extents of lightness perceptibility. In a similar style, the a* and b* components are defined as:

$$a^* = 500\left\{ f\left(\frac{P}{P_n}\right) - f\left(\frac{Q}{Q_n}\right)\right\} \tag{3}$$

$$b^* = 200\left\{ f\left(\frac{Q}{Q_n}\right) - f\left(\frac{R}{R_n}\right)\right\} \tag{4}$$

Where $\{P_n, Q_n, R_n\}$ is the achieved white point and $\{P, Q, R\}$ is obtained from the $\{R, G, B\}$ colors, as follows:

$$\begin{bmatrix} X \\ Y \\ Z \end{bmatrix} = \frac{1}{0.17697} \begin{bmatrix} 0.49 & 0.31 & 0.20 \\ 0.17697 & 0.8124 & 0.01063 \\ 0.00 & 0.01 & 0.99 \end{bmatrix} \begin{bmatrix} R \\ G \\ B \end{bmatrix} \tag{5}$$

3.2.2. Fuzzy C-Means Clustering

Clustering is a way of segregating groups of objects that share a common set of attributes. Fuzzy clustering discoveries partitions such that objects within each cluster are as close to each other as possible by assigning fractional membership degrees in numerous neighboring clusters.

Fuzzy c-means considers one object to belong to two or more clusters. It involves a two folds iterative process:

1. The calculation of the centers of the clusters.
2. Allocation of points to these centers employing Euclidean distance measure.

This process is iterated for the time the cluster centers are stabilized. The fuzzy c-means impose a direct constraint on the fuzzy membership function [4, 10] related to each point, that is, the addition of memberships of all data points equals to one.

$$\sum_{k=1}^{P} \mu_p(x_q) = 1, \quad q = 1, 2, 3, \ldots, Q \tag{6}$$

Where P is the number of identified groups, Q is the number of data points, and $\mu_p(x_q)$ is a function that returns the degree of membership of x_q in the q-th cluster.

This algorithm is organized with the minimization of a characteristic function, expressed as:

$$f = \sum_{p=1}^{P} \sum_{q=1}^{Q} \left[\mu_p(x_q)\right]^m \left\| x_q - c_p \right\|^2, \quad 1 \le m < \infty \tag{7}$$

Where x_q is the q-th data point, m is the fuzzification constraint, c_p is the center of the p-th cluster, ||*|| is any norm representing the similarity between any

designated data and the center, m is any real number greater than 1.

Fuzzy partitioning is accomplished over an iterative optimization of the characteristic function expressed by Equation (8) with the update of membership $\mu_p(x_q)$ and the cluster centers c_k, expressed as:

$$\mu_p(x_q) = \frac{1}{\sum_{k=1}^{C}\left(\frac{\|x_q - c_p\|}{\|x_q - c_k\|}\right)^{\frac{2}{m-1}}} \tag{8}$$

And

$$c_k = \frac{\sum_q \left[\mu_k(x_q)\right]^m x_q}{\sum_q \left[\mu_k(x_q)\right]^m} \tag{9}$$

This iteration will be terminated when $\max_{pq}\left(\left|\mu_p(x_q)^{(k+1)} - \mu_p(x_q)^{(k)}\right|\right) < \lambda$, where λ is a termination criterion between 0 and 1, whereas k are the iteration steps. This process converges to a local minimum of the characteristic function f.

4. Results and Discussion

The effectiveness of the proposed approach has been validated over various satellite constellations at numerous environments. The investigations were performed over an Intel® Core ™ i-5 2.2 GHz laptop with 4 GHz RAM using Visual C++.

Since Al-Ahsa has undergone a radical alteration in the demographical features over the preceding three decades, an area of about 1,500 km^2 throughout Hofuf and the surrounding suburbs, has been chosen for change detection analysis. The satellite images from Landsat 5 TM and Landsat 7 ETM have been collected for the evaluation period (1984 to 2018). The attained images have been analysed by colour segmenting over CIE colour model and processed by root-mean-square (rms) scaling [9]. When a satellite image is exposed in the input, the system provides the resulting output highlighting the image with the given features for the land use information in number of pixels and in hectares. The resolution of the original image was 1500×1779 pixels and has been converted into 500× 593 pixels during processing. The land class distribution of the study area for different years during the period 1984-2018 is shown in Figure 2.

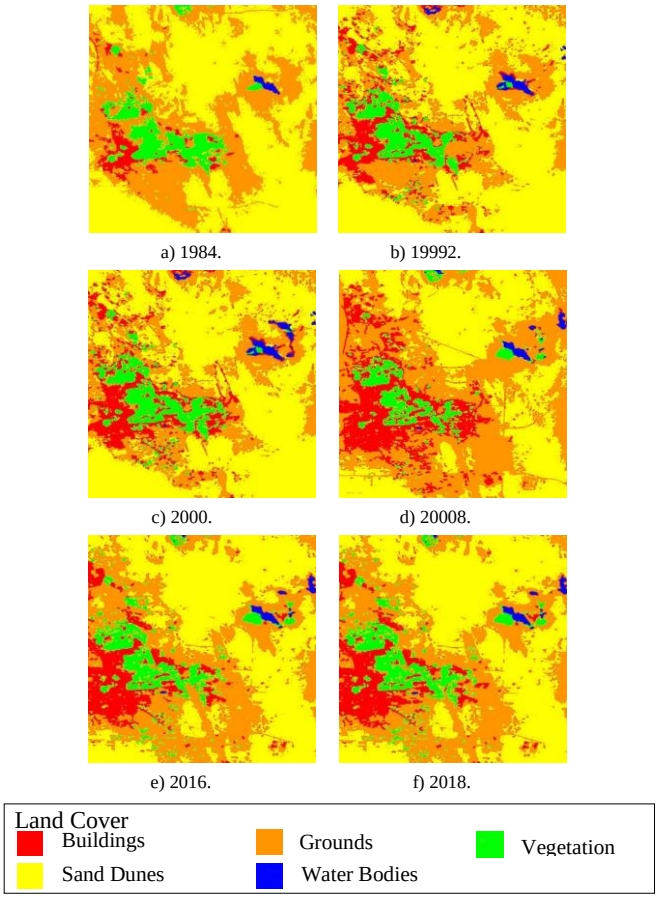

Figure 2. Land class distribution map of the study area.

On attaining the statistical evidence for every class information, images have been classified by employing fuzzy c-means algorithm. The five basic land cover classes are identified as: buildings, grounds, vegetation, sand dunes, and water bodies. Buildings are all the built-up space or urban areas of man-made structures which include residential, commercial, industrial areas. Grounds are the land covers which include all types of open space, sand and bare soil with no vegetation or uncultivated land. Vegetation include all types of land cover with trees, grasslands, gardens, parks, playgrounds, agricultural lands and crop fields. Sand dunes are the zones of sands in a desert formed by wind. Water bodies include all sorts of water reservoirs like ponds, lakes, cannels and coastal water.

The statistics of the attained coverage of each land cover feature throughout the investigated periods (1984, 1992, 2000, 2008, 2016 and 2018) is presented in hectare (ha) and percentage, is furnished in Table 1. Experimental results indicate that the sand dunes class is the largest and the most prevailing among all the land covers. It occupies an area ranging from 115,586 ha (54.32%) to 101,537 ha (47.72%) from 1984 to 2018, with a substantial wavering throughout the evaluation period. The statistics reveal that the coverage of grounds class is the second highest, ranging from 77,244 ha (36.3%) to 73,740 ha (34.65%). The total coverage of these two land covers,

which represent the geographical identity, is more than 80% in all estimated periods. The gain or loss of land cover has been calculated by dividing the discrepancy between the final period (2018) and initial period (1984) over the initial period (2018). So the ensuing gain indicates that the Buildings class exhibits the maximum alteration in land cover (233%). This study is in line with the findings of other preceding investigations [2, 25].

The land coverage of vegetation class has been estimated as 13,032 ha in 1984 and culminated to 15,137 ha in 2018; indicating a significant gain of 16.2%. The buildings coverage which indicate the urban region has been estimated as 6,295 ha in 1984 and extended up to 20,965 ha by 2018 owing to urban spread. The urban region expanded with a gain of 233% for the last three decades and consequently reduced the ground land or Bare soil coverage from 77,244 ha to 73,740 ha during the period from 1984 to 2018. Finally, although the land coverage of water bodies occupies minor percentage of the land cover but nevertheless it exhibits a significant growth (123%), expanding from 635 ha to 1,413 ha. The chronological changes in different features of land cover during the period 1984-2018 is illustrated in a bar diagram, as shown in Figure 3.

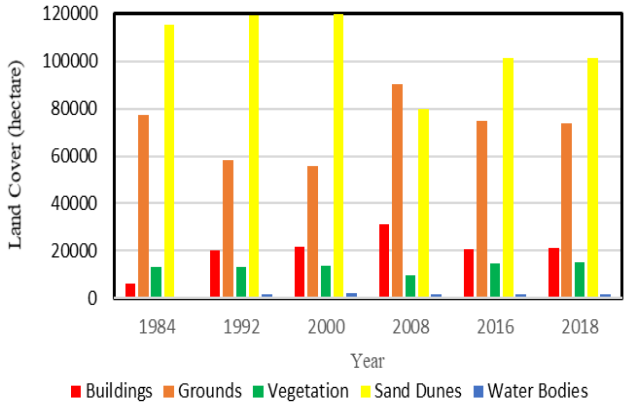

Figure 3. Chronological changes in different features of land cover during the period 1984-2018.

Vegetation and water bodies are the most important components for agricultural development. The statistics reveal a vibrant spatial intermittence in vegetation cover class. It exhibits an abrupt reduction of the area from 13,535 ha in 2000 to 9,701 ha in 2008 (- 28.3%). This land cover shrinkage happened due to the urban sprawl with an enormous gain in the land coverage of buildings that augmented from 21,583 ha in 2000 to 31,420 ha in 2008, gaining about 45.6%.

To detect the changes in vegetation cover, this research uses the change vector analysis which requires two parameters: the magnitude of alteration describing the amount of change and the angle indicating the change dimension. The change vector of each pixel comprises two constituents: Normalized Difference Vegetation Index (NDVI) and Bare Soil Index (BSI) expressed by the following equations [26]:

$$NDVI = \frac{(NIR - R)}{(NIR + R)} \tag{10}$$

$$BSI = \frac{((SWIR + R) - (NIR + B))}{((SWIR + R) + (NIR + B))} \tag{11}$$

Where *NIR*, *R*, *SWIR* and *B* are the spectral reflectance measurements attained in the near-infrared, red, short wave infrared and blue regions (band 4, 3, 5 and 1 in Landsat ETM+ image). The magnitude M and direction θ of change vector are achieved by the following expressions:

$$M = \sqrt{(NDVI_2 - NDVI_1)^2 + (BSI_2 - BSI_1)^2} \tag{12}$$

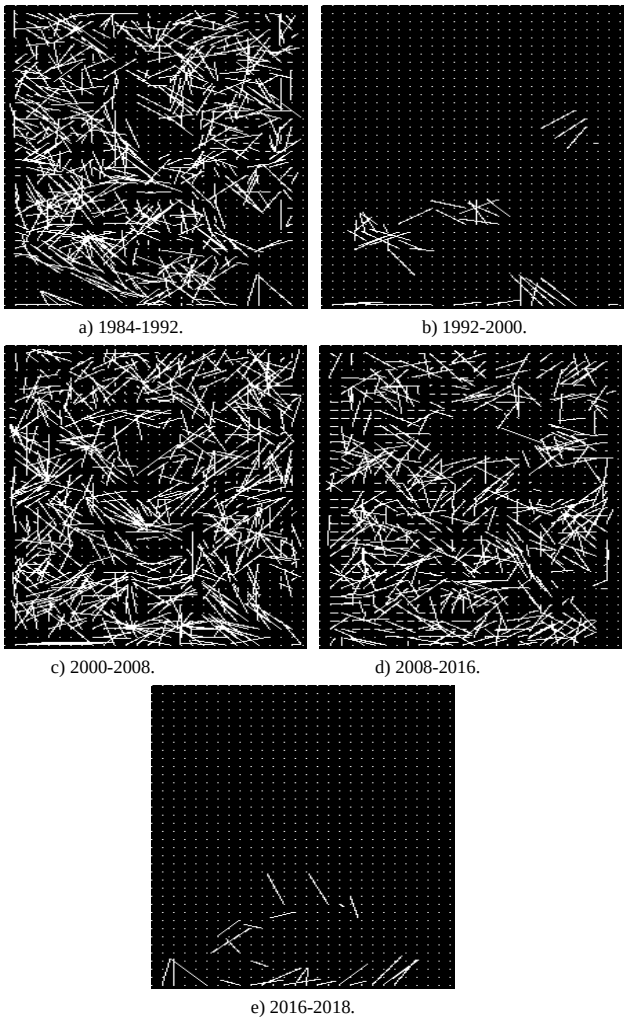

a) 1984-1992. b) 1992-2000. c) 2000-2008. d) 2008-2016. e) 2016-2018.

Figure 4. Motion field during the period 1984-2018.

Table 1. Land cover information in hectare (ha) and percentage (%) during the period 1984-2018.

Land Covers	1984	1992	2000	2008	2016	2018	Gain/ Loss
Buildings	6,295 (2.96%)	20,114 (9.45%)	21,583 (10.14%)	31,420 (14.76%)	20,460 (9.61%)	20,965 (9.85%)	233%
Grounds	77,244 (36.3%)	58,082 (27.3%)	55,636 (26.15%)	90,211 (42.39%)	74,901 (35.2%)	73,740 (34.65%)	-4.5%
Vegetation	13,032 (6.12%)	13,345 (6.27%)	13,535 (6.36%)	9,701 (4.56%)	14,697 6.9%)	15,137 (7.11%)	16.2%
Sand Dunes	115,586 (54.32%)	11,9531 (56.17%)	119,776 (56.28%)	80,026 (37.61%)	101,322 (47.61%)	101,537 (47.72%)	-12.2%
Water Bodies	635 (0.3%)	1,720 (0.81%)	2,263 (1.06%)	1,433 (0.67%)	1,413 (0.66%)	1,413 (0.66%)	123%

$$\theta = \tan^{-1}\left(\frac{BSI_2 - BSI_1}{NDVI_2 - NDVI_1}\right) \tag{13}$$

Where $NDVI_1$ and $NDVI_2$ are the digital number of each pixel in the *NDVI* image on date 1 and 2, BSI1 and BSI2 are the digital number of each pixel in the bare soil index image on date 1 and date 2. This research computes the magnitude and direction of change vector to detect the alteration of vegetation cover. The change direction is shown with the motion field, as shown in Figure 4. Although no appreciable change occurred during 1992-2000 and 2016-2018 but there was tremendous change in 1984-1992, 2000-2008 and 2008-2016. The spatial change in hectare for Vegetation and Water Bodies classes is presented in Figure 5.

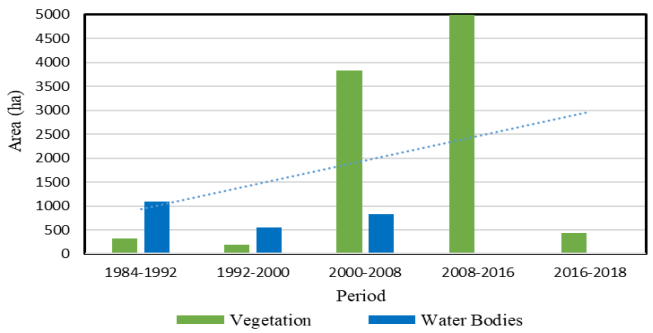

Figure 5. The spatial change in hectare for vegetation and water Bodies classes.

Although a slow extension happened in vegetation cover during 1984 to 2018 and the vegetation trend line shows an overall increasing order, but obviously there is an abrupt change in the vegetation class during 2000-2008 and 2008-2016. Similarly, no appreciable urban expansion occurred during the period 2016-2018 (according to Table 1). On the contrary initiatives were taken for agricultural development which spreads the coverage of vegetation feature of the land class. Moreover, a severe reduction in the coverage of sand dunes has been identified after 2008 that can be allocated to land management purposes.

In order to evaluate the accuracy of the classification outcomes, error matrices have been developed and examined for this study. This research performs four error measures. These are

1. Producer's accuracy.
2. User's accuracy.
3. Errors of commission.
4. Errors of omission.

The producer's accuracy measures the probability that a pixel in a given class is correctly classified. The user's accuracy calculates the probability that a pixel assumed to be in a certain class truly belongs to that class. It is the ratio of the correctly assumed pixels to the total number of pixels in the image assumed to be in a certain class.

The errors of commission, which indicates the false positives, is defined as the fraction of pixels that were assumed to be in a class but do not belong to that class. The errors of omission, which indicate the false negatives, are defined as the fraction of pixels that belong to a class but were assumed to be in a different class. The producer's accuracy and user's accuracy for each land cover classes are furnished in Table 2. The errors of commission and errors of omission for each classes are presented in Table 3.

The kappa coefficient computes the agreement between classification and truth values and is expressed by the following equation:

$$k = \frac{\sum_{j=1}^{J} x_{j,j} - \left\{\sum_{j=1}^{J}(T_j P_j)\right\} / M}{M - \left\{\sum_{j=1}^{J}(T_j P_j)\right\} / M} \tag{14}$$

Where: j is the class number, M is the total number of classified items compared to truth values, $x_{j,j}$ is the number of items belonging to the truth class j that have been identified as class j, T_j is the number of predicted items belonging to class j, P_j is the number of truth items belonging to class j.

The overall accuracy of land cover classification and kappa coefficients during the period 1984-2018 is presented in a bar diagram as shown in Figure 6. The effectiveness of the proposed method has been validated over calculating the accuracies for the five dominant features: Buildings, Grounds, Vegetation, Sand Dunes, and Water Bodies. The proposed Color Segmented Fuzzy Clustering (CSFC) method performed better results for Buildings, Vegetation and Water Bodies images. The relative performances in different approaches like ReliefF, Simulating Annealing (SA), SVM, Particle Swarm Optimization (PSO), GA, GA with Tabu Search (GATS) and the proposed CSFC have been justified in terms of their accuracies and furnished in a bar diagram, as shown in Figure 7. Although image enhancement techniques have been applied, but buildings and grounds images do not produce more accuracy due to overlapping with sand dunes images. This limitation has been greatly overcome in this investigation with the inclusion of the overlapped membership functions of the distinct categories to detect overlapped and occluded objects in images.

Table 2. Error matrices for land cover during the period 1984-2018.

	Producer's Accuracy						User's Accuracy					
	1984	1992	2000	2008	2016	2018	1984	1992	2000	2008	2016	2018
Buildings	91.6	94.7	95.0	95.6	93.3	93.7	91.8	94.3	94.7	95.7	92.7	93.2
Grounds	95.3	96.2	92.1	95.4	93.0	93.2	95.2	92.7	92.2	95.4	93.0	93.2
Vegetation	95.5	97.7	98.7	98.0	99.3	99.3	95.9	97.7	98.8	98.0	99.3	99.3
Sand Dunes	97.2	96.9	96.9	96.2	95.7	95.9	97.3	98.8	96.9	96.2	95.8	96.0
Water Bodies	93.2	96.7	97.8	95.8	97.8	97.8	94.3	97.1	97.9	95.8	97.8	97.6

Table 3. Errors of commission and Errors of omission for land cover during the period 1984-2018.

	Errors of Commission						Errors of Omission					
	1984	1992	2000	2008	2016	2018	1984	1992	2000	2008	2016	2018
Buildings	9.16	5.67	5.26	3.82	7.20	6.81	8.31	5.28	4.94	3.70	6.76	6.25
Grounds	4.80	7.33	7.75	4.32	6.98	6.77	4.62	3.78	7.85	4.38	6.98	6.76
Vegetation	4.05	2.32	1.13	1.65	0.63	0.62	4.40	2.27	1.24	1.94	0.60	0.62
Sand Dunes	2.64	1.17	3.08	3.84	4.14	3.96	2.71	3.09	3.07	3.78	4.24	4.10
Water Bodies	5.64	2.93	2.07	4.08	2.11	2.14	6.75	3.37	2.16	4.14	2.18	2.15

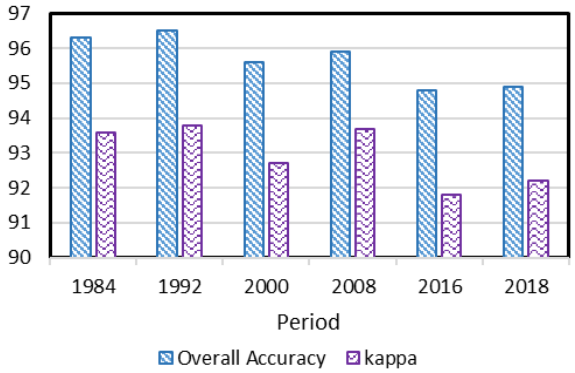

Figure 6. The overall accuracy and kappa coefficient for land cover classification during the period 1984-2018.

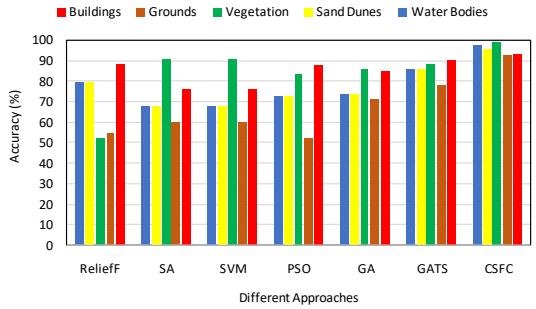

Figure 7. Accuracies of dominant classes for different approaches.

The land cover classification employing remote sensing and GIS strategies in tandem with image processing and machine learning approaches paved a beneficial tool to describe spatial and chronological alterations in land cover in Al-Ahsa. Landsat images are analyzed by Fuzzy c-means classification with overlapping membership functions. The major findings of this study are:

- During the last three decades (1984-2018), the buildings or built-up area has substantially increased 233% and most of it had augmented during 1992-2008.
- The reduced growth of buildings in 2016-2018 clearly indicates the saturation of built-up area of Al-Ahsa region.
- Most of the urban development occurred on grounds or bare lands and a minor occupation in vegetation and cultivated land was observed during 2008 due to significant urban sprawl.
- In spite of urban development, both Vegetation and Water Bodies coverage still increased to 16.2% and 123% respectively, during the period 1984-2018, which is an indication of environmental sustainability.

4. Conclusions

This article explores the land cover classification and chronological variation of land use change pattern of Al-Ahsa, the eastern province of Saudi Arabia through Fuzzy c-means clustering. The proposed land cover classification has been compared with other existing popular land cover classification methods like GA, GATS, SA, SVM, PSO strategies. The evaluations are performed with communal strategies for enhanced precision and high quality assessment constraints. Satellite images are deliberated in five distinct classes: Buildings, Grounds, Vegetation, Sand Dunes, and Water Bodies for endorsement of categorized output. Images are assessed in terms of producer's accuracy and user's accuracy, commission, omission and overall accuracy. This classification method offers more suitable outcomes in terms of speed when compared similar counterpart approach like the minimum distance classifier because the minimum distance classifier is substantially sluggish owing to additional computations associated with the system. These analysis and investigations have been carried out with image resolution of 500×683 pixels during the phase of processing. This sort of investigation will enhance agricultural development over crop monitoring, irrigation, harvesting and urban development with dissemination of land cover information.

Acknowledgments

The authors extend their appreciation to the Deputyship for Research and Innovation, Ministry of Education in Saudi Arabia for funding this research work through the project number IFT20121.

References

[1] Aljoufie M., Zuidgeest M., Brussel M., and Maarseveen M., "Spatial-Temporal Analysis of Urban Growth and Transportation in Jeddah City, Saudi Arabia," *Cities*, vol. 31, pp. 57-68, 2013.

[2] Almadini A. and Hassaballa A., "Depicting Changes in Land Surface Cover at Al-Hassa Oasis of Saudi Arabia using Remote Sensing and GIS Techniques," *PloS ONE*, vol. 14, no. 11, pp.

1-19, 2019.

[3] Alqurashi A. and Kumar L., "Land Use and Land Cover Change Detection in the Saudi Arabian Desert Cities of Makkah and Al-Taif Using Satellite Data," *Advanced Remote Sensing*, vol. 3, no. 3, pp. 106-119, 2014.

[4] Alzahrani A., Bhuiyan M., and Akhter F., "Detecting COVID-19 Pneumonia over Fuzzy Image Enhancement on Computed Tomography Images," *Computational and Mathematical Methods in Medicine*, vol. 2022, no. 1043299, pp. 1-12, 2022.

[5] Al-Gaadi K., Samdani M., and Patil V., "Assessment of Temporal Land Cover Changes in Saudi Arabia using Remotely Sensed Data," *Middle-East Journal of Scientific Research*, vol. 9, no. 6, pp. 711-717, 2011.

[6] Al-Harbi K., "Monitoring of Agricultural Area Trend in Tabuk Region-Saudi Arabia using Landsat TM and SPOT Data," *The Egyptian Journal of Remote Sensing and Space Science*, vol. 13, no. 1, pp. 37-42, 2010.

[7] Amini S., Saber M., Rabiei-Dastjerdi H., and Homayouni S., "Urban Land Use and Land Cover Change Analysis Using Random Forest Classification of Landsat Time Series," *Remote Sensing*, vol. 14, no. 11, pp. 2654, 2022.

[8] Badr E. and Al-Naeem A., "Assessment of Drinking Water Purification Plant Efficiency in Al-Hassa, Eastern Region of Saudi Arabia," *Sustainability*, vol. 13, no. 11, pp. 1-17, 2021.

[9] Bhuiyan A. and Khan A., "Image Quality Assessment Employing RMS Contrast and Histogram Similarity," *The International Arab Journal of Information Technology*, vol. 15, no. 6, pp. 983-989, 2018.

[10] Cox E., *Fuzzy Modeling and Genetic Algorithms for Data Mining and Exploration*, New Delhi, 2015.

[11] Fan H., Wei Q., and Shui D., "The Method of Extracting Land Classification Information by HRI-RefineNET Model," *IEEE Access*, vol. 8, pp. 599-610, 2020.

[12] Häme T., Sirro L., Kilpi J., Seitsonen L., Andersson K., and Melkas T., "A Hierarchical Clustering Method for Land Cover Change Detection and Identification" *Remote Sensing*, vol. 12, no. 1751, pp. 1-22, 2020.

[13] Hemati M., Hasanlou M., Mahdianpari M., and Mohammadimanesh F., "A Systematic Review of Landsat Data for Change Detection Applications: 50 Years of Monitoring the Earth," *Remote Sensing*, vol. 13, no. 2869, pp. 1-18, 2021.

[14] Khurana M. and Saxena V., "Green Cover Change Detection using a Modified Adaptive Ensemble of Extreme Learning Machines for North-Western India," *Journal of King Saud University-Computer and Information Sciences*, vol. 33, no. 10, pp. 1265-1273, 2021.

[15] Lima R. and Marfurt K., "Convolutional Neural Network for Remote-sensing Scene Classification: Transfer Learning Analysis," *Remote Sensing*, vol. 12, pp. 1-21, 2019.

[16] Macarringue L., Bolfe É., and Pereira P., "Developments in Land Use and Land Cover Classification Techniques in Remote Sensing: A Review," *Journal of Geographic Information System*, vol. 14, no. 1, pp. 1-28, 2022.

[17] Memon N., Parikh H., Patel S., Patel D., and Patel V., "Automatic Land Cover Classification of Multi-Resolution Dualpol Data using Convolutional Neural Network (CNN) Remote Sensing Applications," *Society and Environment*, vol. 22, pp. 1-7, 2021.

[18] Nasiri V., Deljouei A., Moradi F., Sadeghi S., and Borz S., "Land Use and Land Cover Mapping Using Sentinel-2, Landsat-8 Satellite Images, and Google Earth Engine: A Comparison of Two Composition Methods," *Remote Sensing*, vol. 14, no. 1977, pp. 1-18, 2022.

[19] Phiri D., Morgenroth J., and Xu C., "Four Decades of Land Cover and Forest Connectivity Study in Zambia-An Object-Based Image Analysis Approach," *International Journal of Applied Earth Observation and Geo-information*, vol. 79, no. 7, pp. 97-109, 2019.

[20] Praticò S., Solano F., Fazio S., and Modica G., "Machine Learning Classification of Mediterranean Forest Habitats in Google Earth Engine Based on Seasonal Sentinel-2 Time-Series and Input Image Composition Optimisation," *Remote Sensing*, vol. 13, no. 4, pp. 586, 2021.

[21] Qian X. and Zhang L., "An Integration Method to Improve the Quality of Global Land Cover," *Advanced Space Research*, vol. 69, no. 3, pp. 1427-1438, 2022.

[22] Rahman M., "Land Use and Land Cover Changes and Urban Sprawl in Riyadh, Saudi Arabia: An Analysis using Multi-Temporal Landsat Data and Shannon's Entropy Index," *The International Archives of the Photogrammetry, Remote Sensing and Spatial Information Sciences*, vol. 41, pp. 1017-1021, 2016.

[23] Rahman M., "Detection of Land Use/Land Cover Changes and Urban Sprawl in Al-Khobar, Saudi Arabia: An Analysis of Multi-Temporal Remote Sensing Data," *ISPRS International Journal of Geo-Information*, vol. 5, no. 2, pp. 15, 2016.

[24] Salam A., "Population and Household Census, Kingdom of Saudi Arabia 2010: Facts and Figures," *International Journal of Humanities and Social Science*, vol. 3, no. 16, pp. 258-263, 2013.

[25] Salih A., "Classification and Mapping of Land Cover Types and Attributes in Al-Ahsaa Oasis, Eastern Region, Saudi Arabia using Landsat-7 Data," *Journal of Remote Sensing and GIS*, vol. 7, no. 1, pp. 228, 2018.

[26] Sanz W., Saa-Requejo A., Díaz-Ambrona C., Ruiz-Ramos M., Rodríguez A., Iglesias E., Esteve P., Soriano B., and Tarquis A., "Normalized Difference Vegetation Index Temporal Responses to Temperature and Precipitation in Arid Rangelands," *Remote Sensing*, vol. 13, no. 5, pp. 840, 2021.

[27] Szwliski R., *Computer Vision: Algorithms and Applications*, London, 2022.

[28] Taani A., AlFanatseh A., Taran A., and ALRashid F., "Monitoring Land use Changes in Al-Hofuf City using Geographic Information System (GIS) and Remote Sensing (RS) Techniques," *European Journal of Scientific Research*, vol. 146, no. 3, pp. 267-283, 2017.

[29] Van T., Tran N., Bao H., Phuong D., Hoa P., and Han T., "Optical Remote Sensing Method for Detecting Urban Green Space as Indicator Serving City Sustainable Development," *Multidisciplinary Digital Publishing Institute Proceedings*, vol. 2, no. 3, pp. 140, 2018.

[30] Xu L., Che Y., Pan J., and Gao A., "Multi-Structure Joint Decision-Making Approach for Land Use Classification of High-Resolution Remote Sensing Images Based on CNNs," *IEEE Access*, vol. 8, pp. 42848-42863, 2020.

[31] Yao Y., Yan X., Luo P., Liang Y., Ren S., Hu Y., Han J., and Guan Q., "Classifying Land-Use Patterns by Integrating Time-Series Electricity Data and High-Spatial Resolution Remote Sensing Imagery," *International Journal of Applied Earth Observation and Geo-information*, vol. 106, no. 102664, pp. 1-18, 2022.

[32] Youssef A., Abu abdullah M., Pradhan B., and Gaber A., "Agriculture Sprawl Assessment using Multi-Temporal Remote Sensing Images and its Environmental Impact, Al-Jouf, KSA," *Sustainability*, vol. 11, no. 15, pp. 4177, 2019.

Ali Alzahrani received his B.Eng. degree in Computer Engineering from Umm Al-Qura University, Makkah, Saudi Arabia, and His M.Sc. and Ph.D. in Computer Engineering from the University of Victoria, BC, Canada, in 2015 and 2018, respectively. He is an Assistant Professor at the Department of Computer Engineering, King Faisal University. His research interests include hardware security, encryption processors, image processing, systems-on-chip and so on.

Al-Amin Bhuiyan graduated from University of Dhaka, Bangladesh and received his Ph. D from Osaka City University, Japan. He is an Associate Professor at the Department of Computer Engineering, King Faisal University, Saudi Arabia. Dr. Bhuiyan lent his teaching and research experiences at several Universities in Japan, Bangladesh and UK. His research interests include image processing, pattern recognition, computer graphics, neural networks, AI, robotic vision, and so on.